

Application of Papoulis-Gerchberg Method in Image Super-resolution and Inpainting

PRIYAM CHATTERJEE¹, SUJATA MUKHERJEE¹, SUBHASIS CHAUDHURI¹ AND GUNA SEETHARAMAN²

¹*Dept. of Electrical Engineering,
Indian Institute of Technology Bombay, India*

²*Air Force Institute of Technology, USA
Email: sc@ee.iitb.ac.in*

In this paper we study the Papoulis-Gerchberg (PG) method and its applications to domains of image restoration like super-resolution (SR) and inpainting. We show that the method performs well under certain conditions. We then suggest improvements to the method to achieve better SR and inpainting results. The modification applied to the SR process also allows us to apply the method to a larger class of images by doing away with some of the restrictions inherent in the classical PG method. We also present results to demonstrate the performance of the proposed techniques.

Received May 2006; revised Feb 2007; accepted May 2007

1. INTRODUCTION

Signal interpolation and extrapolation methods are subjects of immense research. In digital form, a signal is stored and represented by a finite number of samples. Interpolation of such a signal is the method of finding out samples between those that are known. This is a highly ill-posed problem since there are infinitely many signals that may have the same samples. In most cases, signals are assumed to be bandlimited. Interpolation then becomes possible if the sampling process satisfies the Nyquist criteria. However, this may not always be true. In such cases, interpolation of signals becomes a non-trivial problem.

Signal interpolation is a requirement for zooming into signals, where a denser representation of the signal may be required. Interpolation techniques are used for image super-resolution where the spacial density of an image is required to be increased. In essence, given some sampled version of an image, we need to find out more samples of the image so that we get a more detailed spatial description. Another application of signal interpolation is in image inpainting. Image inpainting uses non-uniform signal interpolation to find sample values over a region where no signal samples are provided. Like super-resolution, the inpainting problem too is numerically ill-posed and the complexity increases

as we attempt to recover sample values over a larger area.

Signal extrapolation, on the other hand, is the method of finding out a signal when only a subset of the signal is available. It is thus extending a signal beyond the range in which the signal is available to us. Signal extrapolation theory has been applied to perform image super-resolution by extrapolating the spectrum beyond the diffraction limit of a finite object [1]. In [2] Slepian uses the prolate spheroidal function-based extrapolation technique making an assumption on the bandlimitedness of the signal. An approach of analytic continuation of a signal from only a known segment was proposed by Harris in [3]. He establishes that, given a finite extent of an object and a continuous but finite portion of the spectrum of the object, the entire spectrum can be generated uniquely using the principle of analytic continuation. This leads to an exact and complete reconstruction of the object spectrum if the measurements are noise free. However, this global method becomes highly unreliable even if a small amount of noise is present in the given portion of the spectrum. An iterative method to signal extrapolation was demonstrated independently by Papoulis [4] and Gerchberg [5]. We present the popular Papoulis-Gerchberg algorithm in Section 2. In Section 3 we present application of the PG method to perform image

super-resolution and some achievable improvements that we propose. Application of the method to image inpainting with certain modifications are presented in Section 4. Results are shown in Section 5. We finally conclude with a word on the scope for further research in Section 6.

2. PAPOULIS-GERCHBERG METHOD

This method of super-resolution is based on the work done independently by Papoulis [4] and Gerchberg [5]. While Gerchberg proposed a method to perform signal reconstruction given the diffraction limit of the signal and a part of the spectrum, the motivation for Papoulis' work was extrapolation of a bandlimited signal from only a part of the original signal, i.e., determination of the transform

$$F(\omega) = \int_{-\infty}^{+\infty} f(t)e^{-j\omega t} dt \quad (1)$$

of a signal $f(t)$ given a finite segment

$$g(t) = f(t)p_T(t), \quad \text{where } p_T(t) = \begin{cases} 1, & |t| \leq T \\ 0, & |t| > T \end{cases} \quad (2)$$

This is shown in Figure 1(c) which is a truncated version of Figure 1(a). The signal extrapolation is carried out by the method of alternate projections [6], iterating alternately between time and spectral domains. The signal $g(t)$ is first low-pass filtered with a cut-off frequency of σ , assuming σ to be the signal bandwidth of $f(t)$. This is illustrated in the formation of $F_1(\omega)$ in Figure 1(f) from $G(\omega) = G_0(\omega)$ shown in Figure 1(d). In the n^{th} iteration this can be expressed as

$$F_n(\omega) = G_{n-1}(\omega)p_\sigma(\omega), \quad p_\sigma(\omega) = \begin{cases} 1, & |\omega| \leq \sigma \\ 0, & |\omega| > \sigma \end{cases} \quad (3)$$

For illustration we show the filter $p_\sigma(\omega)$ to be an ideal one, but one is free to select an appropriate low pass filter $p_\sigma(\omega)$. The inverse function of $F_1(\omega)$ is then computed as $f_1(t)$ (Figure 1(e)). This results in a reduction of the error signal $|f(t) - f_1(t)|^2$ outside the known segment of the signal. This follows from Parseval's theorem. However, the signal $f_1(t)$ does not match the observed signal $g(t)$ in the region $[-T, T]$. This part of the signal is then restored to the original known segment forming the function $g_1(t)$ for the next iteration as is shown in Figure 1(g). The resultant change in the spectral domain due to introduction of higher frequency components can be seen in Figure 1(h). Generalizing this for the n^{th} iteration we get

$$g_n(t) = f_n(t) + [f(t) - f_n(t)]p_T(t) = \begin{cases} g(t), & |t| \leq T \\ f_n(t), & |t| > T \end{cases} \quad (4)$$

This process is then iterated with the new $g_1(t)$ thus formed. In each iteration the mean square error of

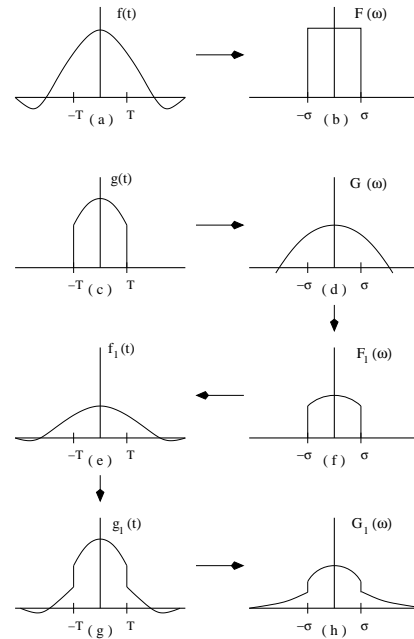


FIGURE 1. Illustration of iterative extrapolation of $g(t)$ using the Papoulis-Gerchberg method. (a) The signal that we want to recover, (b) spectrum of the signal, (c) the time-limited available signal $g(t) = g_0(t)$ used as the initial estimated signal, (d) spectrum of (c), (e) time domain signal from (f), (f) low-pass filtered spectrum of (d), (g) portion of (c) reinstated in (e), (h) spectrum of (g).

the extrapolated signal is reduced [4]. Hence with successive iterations the generated extrapolated signal approaches the desired signal $f(t)$. Convergence of the method is guaranteed and is shown in [4]. However, the process requires an infinite number of iterations. If we stop after r iterations, the reconstructed signal is given by $f_r(t)$ instead of $f(t)$. Also, in practice, the measured data $g(t) = g_0(t)$ will contain error. The propagation of this measurement error can be controlled by early termination of the iterative process [5, 7]. The process also assumes the signal $f(t)$ to be bandlimited, but it is found that the method works reasonably well for signals with sufficiently low energy in their higher frequency components.

3. APPLICATION TO SUPER-RESOLUTION

3.1. Previous work

Super-resolution (SR) refers to the process of producing a high spatial resolution image from one or more low resolution (LR) observations. The super-resolution processing includes three main tasks: an alias-free upsampling of the image, thereby increasing the maximum spatial frequency, and removing degradations that arise during the image capture, viz., blur and noise. In effect, the super-resolution process tries to generate the missing high frequency components and

minimize aliasing, blur and noise. This has been a field of intense research and many different methods have been proposed to obtain high resolution images. The methods differ widely in their choice of domain (spatial, spectral or even both), in the choice of the observation model used, in the method of capturing low resolution images, in the choice of number of low resolution images required and also in the choice of cues that are used to extract information from images. Resolution enhancement using a multiple-aperture camera system has been carried out by Komatsu *et al.*[8]. In this the authors use different aperture systems to acquire multiple LR images. An iterative algorithm is used for alternate registration and reconstruction. Capel *et al.* [9] use different methods of image registration and then go on to estimate the HR image using maximum likelihood estimation (MLE), Maximum a-priori (MAP) estimation with priors like Gaussian Markov random field (MRF) and Huber MRFs. Rajan *et al.* [10, 11] use blur as a cue for super-resolution. They model the HR image and the blur processes as separate independent MRFs. The HR space variant blur and SR image are estimated using a MAP estimator. They also show how MRF models are well suited for modeling the structural information in the form of surface normal. The shape from shading problem has also been used for restoration of an HR image in [10]. In [12, 13], Joshi *et al.* make use of zoom as a cue to perform super-resolution. They consider linear dependency of pixels in a neighborhood of the HR image and model this using a simultaneous auto-regressive (SAR) model. This SAR model is then used as a prior to perform super-resolution. In [14] the authors extend the theory of kernel regression to derive a generalized kernel regression method which successfully performs super-resolution from single and multiple low resolution frames as well as image denoising. Under this framework, the Bilateral filter becomes special case of their kernel regression method.

Researchers have also attempted to solve the super resolution problem by using learning based techniques. These methods try to recognize local features of a low resolution image and then try to retrieve the most likely high frequency information from the given training samples. They try to re-create the HR image from just a single SR image by making use of a image database that is used as a training set. Freeman *et al.* [15] describe image interpolation algorithms which use a database of training images to create plausible high frequency details in zoomed images. In [16], Baker and Kanade develop a super-resolution algorithm by modifying the prior term in the cost function to include the results of a set of recognition decisions, and call it as recognition based SR or “hallucination”. Their prior enforces the condition that the gradient of the HR image should be equal to the gradient of the best matching training image. In [17], Candocia *et al.* address the ill-posedness of the SR problem by assuming that

the correlated neighbors remain similar across scales, and this priori information is learnt locally from the available image samples across scales. When a new image is presented, a kernel that best reconstructs each local region is selected automatically and the super-resolved image is reconstructed by simple convolution operation. In [18], Jiji *et al.* propose a single frame, learning based SR restoration technique by using the wavelet domain to define a constraint on the solution. Wavelet coefficients at finer scales of the unknown HR image are learnt from a set of HR images that are used as a training database. This learnt image is further used for regularization while super-resolving the image. An appropriate smoothness prior is used with discontinuity preservation in addition to the wavelet based constraint to estimate the HR image. This method was further improved by the use of contourlets in [19] to capture edges better and hence results in better reconstruction of images. Surveys of various SR techniques have been presented in [20, 21, 22, 23, 24].

3.2. SR using PG method

The Papoulis-Gerchberg algorithm has been used in a modified form by Vanderwalle *et al.* in [25] to super-resolve images when multiple low-resolution registered images are available. We restrict ourselves to the case when only a single LR image is available. The initial image is thus a higher dimensional grid where the values of some pixels are known and some are unknown. The unknown pixel values are initially set to zero. In the next step, the image is passed through a low pass filter with a normalized cut-off frequency of σ , which is assumed to be the maximal allowable frequency. This effectively results in blurring of the image and the unknown pixels obtain some values. But, the known pixel values have also undergone changes as a result of the filtering. In the next step, the original values of the known pixels are restored, creating high frequency components. The whole process is repeated. Figure 2 shows the reconstructed image after one such iteration of the method. Figure 3 compares the output of the method after 50 iterations with that of the standard bicubic interpolation.

Though the method is quite fast it has some drawbacks. Due to the steep cut-off in the frequency domain, the resultant HR image has ringing artifacts near the edges. Also, it relies heavily on the fact that the measured (known) pixel values are the values that are to be obtained in the reconstructed high resolution image. In other words, it assumes that the low resolution images are downsampled versions of the expected high resolution image without any low-pass (averaging) filtering. Moreover, they should also be totally free from noise perturbations. Hence, it is not able to compensate effectively for blur and noisy measurement of data. Figure 3 demonstrates these drawbacks. In Figure 3(a) we have a fairly good quality

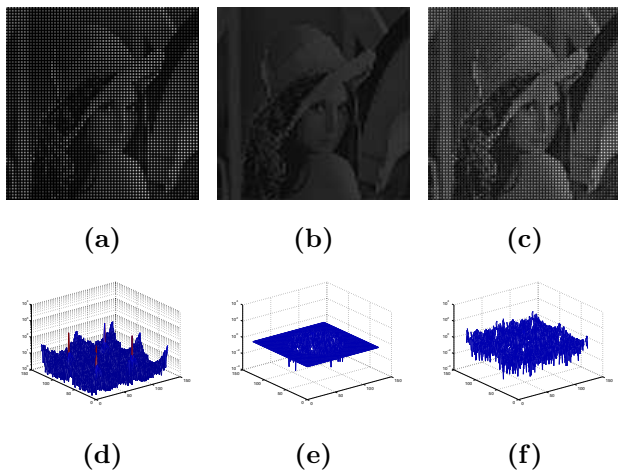


FIGURE 2. (a) The starting of iteration 1 with the HR grid partly filled with the given LR data, (b) image after low-pass filtering with a normalized cut-off frequency of 0.6, (c) image after known pixel values are reset to original values. Spectra in log scale (d) of (a), (e) of (b), and (f) of (c). Notice that the spurious peaks at the higher frequency regions in (d) reduce in (e) due to the spatial filling-in process. This increases again in (f) and the process continues.

LR image, and Figure 3(b & c) show corresponding results of interpolation using bicubic and PG methods, respectively. One may notice that the PG method offers a better result. This can be seen as sharper features near the nose, eyes and freckles. In Figure 3(d) we show a poor quality LR image. The input image is quite blurred. Hence the corresponding HR reconstructions in Figure 3 (e & f) are poor. The PG method offers no help as it assumes correct pixel values on the LR grid. Similarly Figure 3(g) shows a noisy LR input image and the corresponding HR reconstructions are shown in Figure 3(h & i). For the same reason, the PG method does not offer a quality reconstruction.

3.3. Modified Papoulis-Gerchberg Method

As mentioned in Section 3.2, the PG method cannot deal with images that are blurred due to averaging during the downsampling process. We now propose an extension which allows the method to be applied to super-resolution of images for which the downsampling process is known. In our experimentation we assume that the low resolution image is formed by averaging and subsampling the high resolution image that we aim to recover. This means that for $2\times$ zooming of an image we assume that every pixel in the low resolution input image is the average of a corresponding 2×2 pixel block of the high resolution image. The classical PG method will not deliver a good result in such a case as shown in Figure 3. This is because we enforce the available pixel values in the LR image to be pixel values in the HR image. This results in an overall blurred HR image.

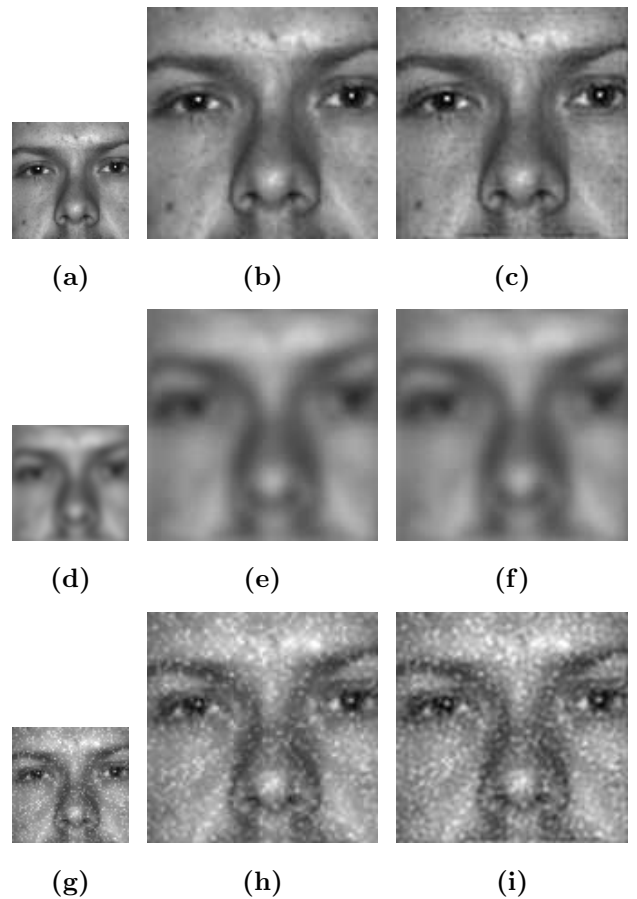


FIGURE 3. (a) A LR face image, (b) $2\times$ zoom of (a) using bicubic interpolation, (c) SR of (a) using PG method, (d) blurred LR image, (e) $2\times$ zoom of (d) using bicubic interpolation, (f) SR of (d) using PG method, (g) noisy LR image, (h) $2\times$ zoom of (g) using bicubic interpolation, (i) SR of (g) using PG method.

We overcome this drawback by introducing a different constraint enforcing part. We want to enforce that the super-resolved image obtained after every iteration of the method conforms to the input LR image. To do this we introduce a back projection part within the PG method. Iterative back projection has been used in image super-resolution by Irani and Peleg [26]. But as opposed to their case, we deal with the case where only a single low resolution image is available.

In our method, after every iteration of the PG method we calculate the error between the LR image and the simulated LR image formed by applying the known decimation model to the obtained SR image. Mathematically, the error ϵ_i can be expressed as

$$\epsilon_i = y - DH z_i \quad (5)$$

where y is the input LR image lexicographically ordered as a vector of size $M^2 \times 1$, D is the $M^2 \times N^2$ decimation matrix (where $N > M$), H is the space invariant (and hence block circulant) blurring matrix of size $N^2 \times N^2$

that we assume to be known to us and z_i is the estimated SR image vector of size $N^2 \times 1$ obtained after the i^{th} iteration of the method. We then compensate for this error in the obtained SR image by adding back the error for each pixel of the simulated LR image to the corresponding block of pixels in the obtained SR image. Thus the image update part for the constraint enforcing term becomes

$$z_i = z_i + P(\epsilon_i). \quad (6)$$

where P is the $N^2 \times M^2$ matrix operator which projects the error in the LR space to the HR space. The compensation is thus done such that the SR image best approximates the desired HR image, under the assumed downsampling process. Ideally we would want $P = (DH)^{-1}$. But being ill-posed in nature, we cannot find a specific P as an inverse to the blurring and upsampling operation. A suitable choice for this would be the pseudo-inverse of DH which has the form $(H^T D^T D H)^{-1} H^T D^T$. This simplifies to $(H^T H)^{-1} H^T D^T$ since all that $D^T D$ does is downsizing followed by upsizing. However, it is still not practically feasible to update the SR estimate using the pseudo-inverse. In our experiments we simply add back the error ϵ_i to each pixel in the corresponding HR block, the size of the block being dictated by the support of the PSF. This back-projection operator, although being simple in approach, is able to perform deblurring of the image. It may be noted here that due to this error compensation in blocks a certain blockiness will be introduced in the SR image obtained at this point. However, this is then taken care of in the low-pass filtering part of the next iteration. A point worth noting here is that the error is calculated in the LR space and is defined as the difference between the available LR image and the simulated LR image formed at every iteration using the parameters of the image formation model. Hence, the error and as a consequence the resultant SR image, are dependent on the accuracy of the image formation model. With every iteration the resultant image gets closer to the desired HR image and can be expected to form the original HR image as the number of iterations approach infinity. Since this is not feasible for practical purposes, we define a terminating condition based on a small tolerable threshold value for error norm ($\|\epsilon_i\|_0$ or $\|\epsilon_i\|_1$) calculated using Equation 5. The algorithm terminates when the error is small enough. The combination of low-pass filtering and back projection of the error ϵ_i in every iteration ensures that the resultant SR image is smooth and approximates one of the possible SR images, under the specified downsampling process. This method can easily be modified to handle any general downsampling process. The proposed process thus generalizes the PG method by making it applicable to any class of images where the downsampling process is known.

We have found that the method performs better than the standard PG method and the results obtained

through bicubic interpolation. The results obtained through different methods are compared in Section 5.

Algorithm 1 Modified PG Method

```

 $y \leftarrow$  Input LR image
 $z \leftarrow$  Sparse HR grid
 $D \leftarrow$  Downsample operator
 $H \leftarrow$  Blur operator
 $P \leftarrow$  Back projection operator
loop
   $Z \leftarrow FFT(z)$ 
   $\hat{Z} \leftarrow$  Low-pass filter  $Z$  with cut-off frequency  $\sigma$ 
   $z \leftarrow IFFT(\hat{Z})$ 

  \* Error calculation *
   $\epsilon \leftarrow y - DH z$ 

  if  $|\epsilon| \leq threshold$  then
    terminate loop
  else
     $z \leftarrow z + P(\epsilon)$ 
  end if
end loop

```

4. APPLICATION TO INPAINTING

4.1. Previous work

Digital Inpainting is the process of predicting the unknown values of pixels so as to remove artifacts like scratches or unwanted objects from an image. Unlike in the case of super-resolution the reference grid is at the same resolution as the observed image. Image inpainting finds use in image and film restoration, texture synthesis, disocclusion and in the entertainment industry. A lot of work has been done to address this problem since Bertalmio *et al.* introduced this term in [27]. Inpainting algorithms based on level lines were proposed by Masnou and Morel [28, 29]. Other authors have taken a variational approach like Ballester *et al.* in [30] and Chen and Shen in [31]. PDE based approaches have also been used by authors in [27, 31]. Oliveira *et al.* [32] propose a fast digital inpainting method using an isotropic diffusion kernel for convolution. They make use of anisotropic kernels to preserve edges. However, their method requires manual intervention to identify pixels where the scratches cross edges in the image. In [33, 34] the authors make use of the Ginzburg-Landau equation to perform image inpainting. A considerable amount of literature is also available where researchers have used projections onto convex sets (POCS) to perform image restoration of this kind. In [35] Hirani and Totsuka present a dual domain iterative method to restore parts of an image. The method requires the users to provide a noise mask and a corresponding mask (repair subimage) and a sample subimage. Their

method makes use of the spectrum of the sample subimage to do scratch removal in the repair subimage. Patwardhan and Sapiro [36] demonstrated a similar method in which they make use of the wavelet transform for inpainting. They do away with the requirement of human provided sample subimage, instead assume that the corrupted portion of the image is as smooth as its neighborhood. They learn the wavelet coefficients from the neighborhood and impose spectral restriction on the noisy sections to restore images. In [37] Chan *et al.* have proposed a framelet-based method. They try to determine the missing framelet coefficients of the unknown pixels from those of the neighborhood. Analysis of some methods for sample recovery in band-limited images and application of adaptive weights conjugate gradient Toeplitz method (ACT) to perform fast image inpainting is presented in [38, 39]. All these methods require projecting the image or a subimage from one domain to another. Since Papoulis-Gerchberg method also follows the same idea, we show that this method can also be used for inpainting purposes.

4.2. Inpainting using PG method

As opposed to super-resolution discussed in the previous section, image inpainting requires filling-in of lesser number of pixels but in many cases the corrupt pixels are contiguous in nature, rendering simple smoothing insufficient. We have applied the Papoulis-Gerchberg algorithm directly to address the issue of image inpainting. To implement this we assume that the pixels to be inpainted are known to us. As is common in inpainting, these are user specified and these pixels are marked as the unknown pixels. Next we fill in values for the unknown pixels using the technique suggested in Section 3.2. We find that the method works considerably well for areas where the region to be inpainted is not very wide. The performance of this method varies with the thickness of the contiguous unknown pixels, even when the number of unknown points remain the same. The problem of inpainting becomes more complex when we encounter larger areas to be inpainted. The PG method, as the results show, is capable of providing a fast and acceptable quality of inpainting when the width of the scratches or areas to be inpainted is relatively thin (say, about 1 to 4 pixels wide).

4.3. Modifications to the PG method

For thicker edges the method does not generate a good result. In such cases the inpainted region displays a ringing effect such as the one experienced in the super-resolution case. We suggest suitable modifications to address this issue.

4.3.1. Filtering with a smooth cut-off

The ringing of the inpainted region is a result of the steep cut-off in the filtering process of the PG method. We introduce a smooth transition band for the cut-off region. The amount of smoothing is controlled by the width of this transition band. A wide transition band would considerably reduce the effect of ringing but it also translates to a poorer low-pass filtering and hence a poorer reconstruction. A trade-off condition is hence to be reached in deciding how smooth we would want our cut-off to be. For our implementation we have used a filter where the slope falls off gently as opposed to the steep cut-off for an ideal filter. This modification does away with the ringing effect to some extent.

4.3.2. Directional filtering

We observe that scratches in images are often highly directional. Hence, we investigate the possibility of using a directional filtering approach to solve the inpainting problem for scratches which have some sort of a directional nature such as the image shown in Figure 7(a). A scratch in one direction introduces higher frequency components in a direction perpendicular to the direction of the scratch. This effect can be seen when we compare the spectrum of the unscratched original image with that of the corrupt image. We modified the filtering process to take advantage of this directional nature of the image corruption. Rather than taking a uniform filtering mask (which was circular in nature for all the above methods), we use a directional filter with two different cut-offs - one for the direction where higher frequency components have been introduced due to the scratch, and another for all other directions. We set a smaller bandwidth for the filter in the direction perpendicular to that of the scratches. This has a greater smoothing effect across the edges of the scratch and allows faster flow of information across the edges into the region to be inpainted.

4.3.3. Extension to different orthogonal bases

Till now our discussion has been restricted to various modifications to the method of filtering in the frequency domain using the discrete Fourier transform (DFT) as the bases. However, it may be noted here that the method will work under any orthogonal transformation maintaining sequence ordering. This encourages us to try out PG method with the DCT bases instead of DFT. DCT implementation using integer arithmetic is also faster than the DFT computation. The choice of DCT also stems from its high energy compaction property. In DCT most of the information about the signal is captured in a few lower frequencies. This leads us to expect that the filtering part in the PG method can be achieved faster as DCT computation is quite fast and we have to deal with only a few DCT coefficients. Taking advantage of the information packing capacity

of DCT, in the low-pass filtering process we simply retain the coefficients near the origin of the transformed image. However, like the filtering in the DFT based PG method, a steep cut-off in the DCT domain also leads to ringing effect due to Gibb's phenomenon. The DCT based method in conjunction with a smooth cut-off filtering process in the DCT domain reduces the ringing effect.

5. RESULTS

5.1. Super-resolution

We applied the algorithm discussed in Section 3.3 on a Lena image of size 128×128 to perform $2\times$ zooming. For this we consider the LR image to have been formed by decimation of the desired 256×256 HR image blurred by simple averaging in a 2×2 window. This defines the forward model of the image formation process and defines the parameters for calculation of the error at every iteration given by Equation 5. We found that the method performs better than the standard PG method. The results obtained are shown in Figure 4.

The image obtained using bicubic and Delaunay interpolation shown in Figure 4(b) and (c) are quite blurred with respect to that obtained using the standard PG method shown in Figure 4(e). We show that the result is further improved using the modified PG method with the deblurring step. This can be seen in Figure 4(f) which is sharper than the other images shown even though the Steering Kernel method provides a better interpolation in the PSNR sense. Note the increase in textural detail of the hat, the sharpness of the lips and nose in the figure with respect to those obtained using other methods even though the PSNR value is less. Results with $3\times$ magnification are shown in Figure 5. The bicubic image in Figure 5(b) is much blurred compared to the output of the standard PG method result shown in Figure 5(c). The result obtained using the deblurring step, shown in Figure 5(d), can be seen to be sharper than the other images, specifically at the scales and leaves of the pineapple.

5.2. Inpainting

In our experiment we first took the Lena image and scratched it arbitrarily with a variable width of 3 to 5 pixels. Subtraction of this image with the original image provided us with an accurate mask of the scratch. This mask is thus the region which is to be inpainted. Then taking all pixels outside this mask as known pixel values we perform the standard PG method to obtain an inpainted image. Similar experiment was carried out with overlaid text of variable font size. The results of the method are shown in Figure 6. Note that while the thinner areas are inpainted without any visual artifacts, this is not the case for the thicker regions.

We then performed inpainting with the proposed modifications. This time we used thicker edges of width

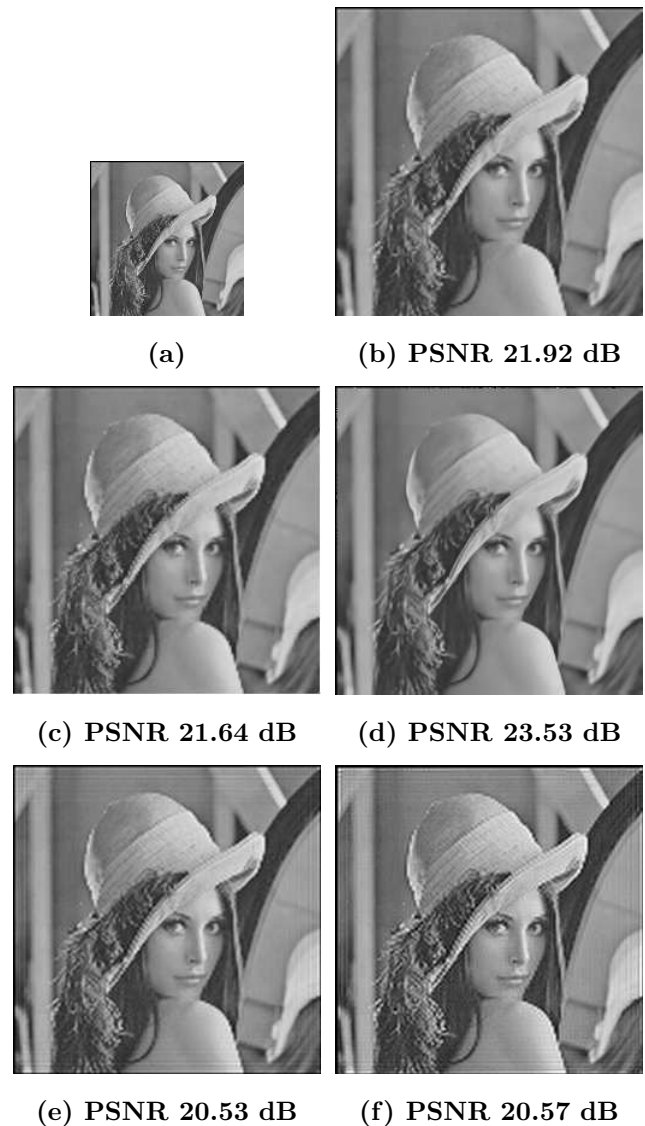


FIGURE 4. (a) Low resolution Lena image formed by averaging and downsampling of a high resolution image, (b) $2\times$ zoomed image using bicubic interpolation, (c) interpolation using Delaunay triangulation, (d) upscaled image using Steering Kernel Regression [14], (e) super-resolved image formed using the standard PG method, (f) super-resolved image formed using the PG method with deblurring.

5 to 7 pixels. The scratches used this time were loosely directional in nature as shown in Figure 7(a). We obtain the scratch mask similar to the method explained above. The resultant inpainted image using the standard PG method with a normalized low-pass filter cut-off of 0.2 is shown in Figure 7(b). Note the ringing effect in the inpainted regions. Next we tried to better this method by using a smooth filter by doing away with the ideal low-pass filter and replacing it with a gradual cut-off. The result obtained shows lesser ringing as pointed out in Figure 7(c). This results in a 0.19dB gain over the

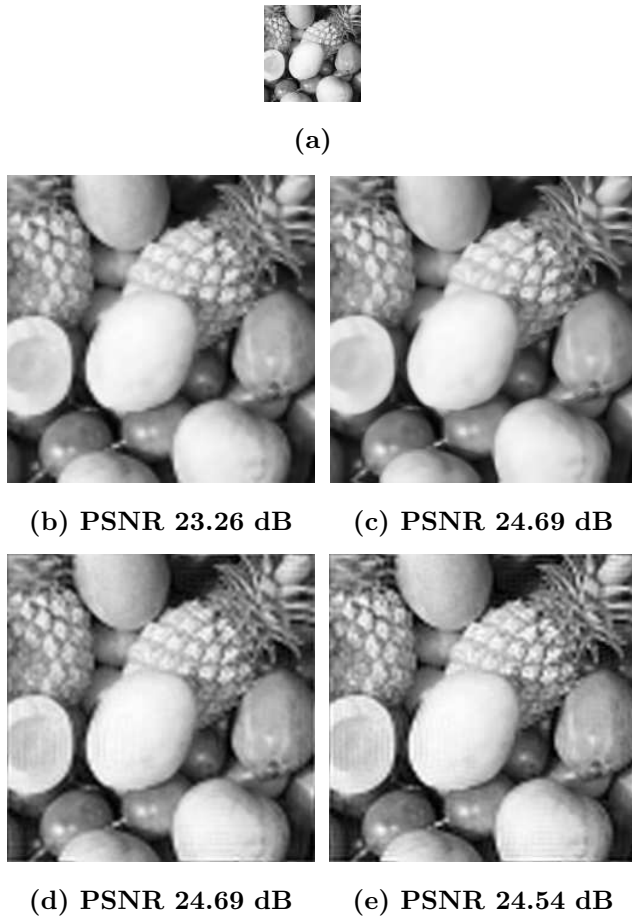


FIGURE 5. (a) Low resolution image formed by 3×3 pixel averaging and downsampling of a high resolution image, (b) $3 \times$ zoomed image using bicubic interpolation, (c) interpolated image using Steering Kernel Regression [14], (d) super-resolved image formed using the standard PG method, (e) super-resolved image formed using the PG method with deblurring.

standard method, as can be seen in Table 1. Figure 7(d) illustrates the result using DCT instead of the DFT, in order to take advantage of the greater information packing density of the DCT. We see that this produces nearly similar results, in terms of quality and PSNR, as compared to using DFT. The result obtained using a smooth cut-off on DCT of the image in the filtering process is shown in Figure 7(e). It shows a 0.29 dB increase in PSNR from that obtained using a simple DCT based filtering. We then show the result obtained using the directional filtering method to take advantage of the directionality of the scratches. In this experiment the lowpass filtering normalized cut-off frequency was kept at 0.1 in the direction perpendicular to that of the scratch and 0.3 elsewhere. The result obtained is shown in Figure 7(f). Notice that the ringing along the smoother areas have reduced. We see that in a PSNR sense all these modifications result in a better

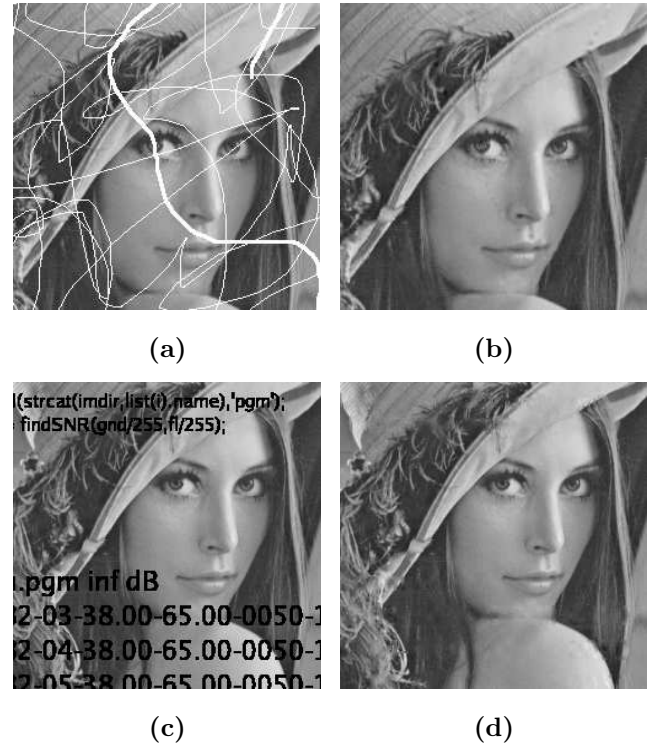


FIGURE 6. Inpainting using the PG method. (a) Lena image with different widths of scratching, (b) Inpainted image of (a), (c) Lena image with varying text sizes, (d) Inpainted image of (c).

| METHOD | PSNR |
|----------------------------------|-------|
| Scratched Image | 20.16 |
| PG Method | 37.67 |
| PG with smooth cut-off | 37.86 |
| PG with directional filtering | 37.72 |
| PG using DCT | 37.65 |
| PG using DCT with smooth cut-off | 37.94 |

TABLE 1. PSNR values of results from different inpainting methods as shown in Figure 7.

inpainted image than that obtained using the standard PG method.

6. CONCLUSION

From the discussions and the results presented above, it is clear that the PG method performs well for super-resolution when one does not have multiple images or any HR training data set. It also does very well in image inpainting. However, it has some severe limitations as illustrated by Figure 3 as it cannot handle noisy data. However, this is quite natural as one does not have multiple images for the purpose of noise smoothing. An early termination of the iterative process as suggested in [4] is one way to stop the propagation of error with future steps. In general, the assumption that exact pixel

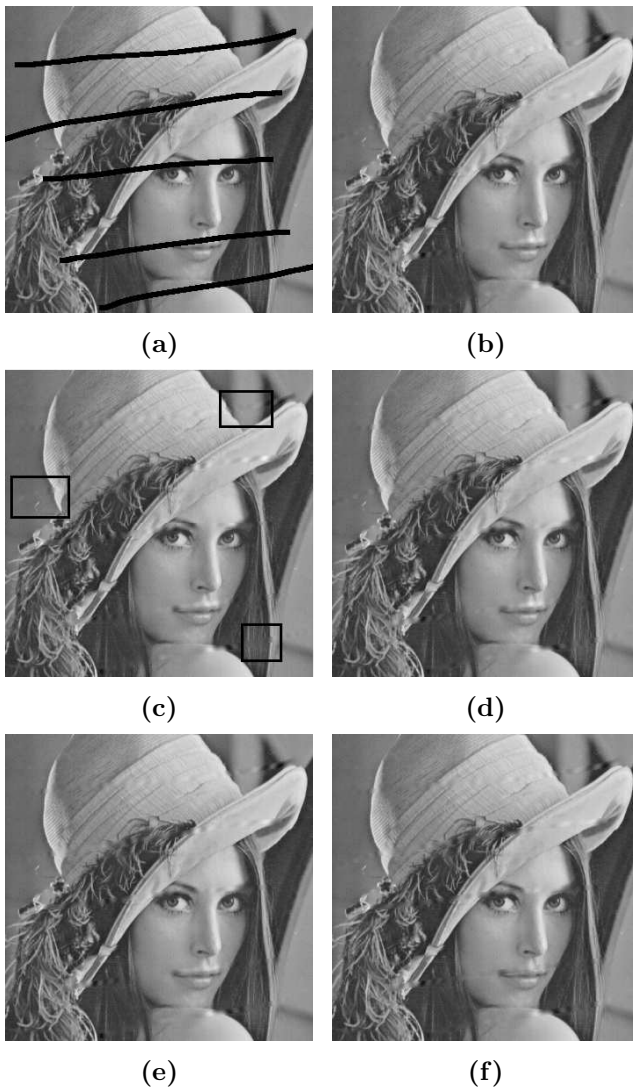


FIGURE 7. (a) Example of a scratched image requiring inpainting. Inpainting using (b) the PG method using a normalized cut-off frequency of 0.2 for the low pass filter, (c) using a smooth filter with a transition band of 30 pixels, (d) the DCT based PG method, (e) DCT based PG with smooth cut-off and (f) directional filtering approach.

values are known is quite restrictive and will not hold true under most downsampling processes. To be able to use the PG algorithm for super-resolution of such low resolution images, we have incorporated a method of undoing the blurring effect, be it known or learnt separately. It may be noted here that although this algorithm is successful in reducing the blurring effect, it still remains sensitive to the presence of noise.

We also show that the PG method can be applied to inpaint a thin area of unknown pixels. We propose modifications to the method to get improved results for thicker scratches. Although these modifications perform better than the standard PG method, they still fail to produce satisfactory results when the scratches

are quite thick, say 8-10 pixel wide. Further research is required to make the algorithm work successfully in such cases. However, the method has its importance due to its speed and simplicity.

ACKNOWLEDGEMENTS

Funding supports from AOARD, USA and ISRO, India are gratefully acknowledged. The authors would also like to thank the reviewers whose suggestions and constructive criticism have brought this paper to its current state. We would also like to extend our gratitude to Hiroyuki Takeda for providing us results of his research to compare against.

REFERENCES

- [1] Sabri, M. S. and Steenart, W. (1978) An approach to band-limited signal extrapolation : The extrapolation matrix. *IEEE Transactions on Circuits and Systems*, **CAS-25**, 74–79.
- [2] Slepian, D. (1978) Prolate spheroidal wave functions, Fourier analysis, and uncertainty- V: The discrete case. *Bell System Tech. J.*, **57**, 1371–1429.
- [3] Harris, J. L. (1964) Diffraction and resolving power. *Journal of Optical Society of America*, **54**, 931–936.
- [4] Papoulis, A. (1975) A new algorithm in spectral analysis and band-limited extrapolation. *IEEE Transactions on Circuits and Systems*, **CAS-22**, 735–742.
- [5] Gerchberg, R. (1974) Super-resolution through error energy reduction. *Optical Acta*, **21**, 709–720.
- [6] Jain, A. K. (2001) *Fundamentals of Digital Image Processing*. Prentice Hall of India Private Limited, New Delhi - 110 001.
- [7] Walsh, D. O. and Nielsen-Delaney, P. A. (1994) Direct method for superresolution. *Journal of Optical Society of America*, **11**, 572–579.
- [8] Komatsu, T., Igarashi, T., Aizawa, K., and Saito, T. (1993) Very high resolution imaging scheme with multiple different-aperture cameras. *Signal Processing: Image Communication*, **5**, 511–526.
- [9] Capel, D. and Zisserman, A. (2003) Computer vision applied to super resolution. *IEEE Signal Processing Magazine*, **20**, 75–86.
- [10] Rajan, D., Chaudhuri, S., and Joshi, M. V. (2003) Multi-objective super resolution: Concepts and examples. *IEEE Signal Processing Magazine*, **20**, 49–61.
- [11] Rajan, D. and Chaudhuri, S. (2003) Simultaneous estimation of super-resolved scene and depth map from low resolution defocused observations. *IEEE Transactions on Pattern Analysis and Machine Intelligence*, **25**, 1102–1117.
- [12] Joshi, M. V. and Chaudhuri, S. (2004) Zoom based super-resolution through SAR model fitting. *Proc. of IEEE Intl. Conf. on Image Processing*, Singapore, August, pp. 1775–1778.
- [13] Joshi, M. V., Chaudhuri, S., and Panuganti, R. (2004) Super-resolution imaging: use of zoom as a cue. *Image and Vision Computing*, **22**, 1185–1196.

- [14] Takeda, H., Farsiu, S., and Milanfar, P. (2007) Kernel regression for image processing and reconstruction. *IEEE Transactions on Image Processing*, **16**, 349–366.
- [15] Freeman, W. T., Jones, T. R., and Pasztor, E. C. (2002) Example-based super-resolution. *IEEE Computer Graphics and Applications*, **22**, 56–65.
- [16] Baker, S. and Kanade, T. (2002) Limits of super-resolution and how to break them. *IEEE Trans. on Pattern Analysis and Machine Intelligence.*, **24**, 1167–1183.
- [17] Candocia, F. M. and Principe, J. C. (1999) Super-resolution of images based on local correlations. *IEEE Trans. on Neural Networks.*, **10**, 372–380.
- [18] Jiji, C. V., Joshi, M. V., and Chaudhuri, S. (2004) Single-frame image super-resolution using learnt wavelet coefficients. *International Journal of Imaging Systems and Technology*, **14**, 105–112.
- [19] Jiji, C. V. and Chaudhuri, S. (2006) Single-frame image super-resolution through contourlet learning. *EURASIP Journal on Applied Signal Processing*, **2006**, 1–11.
- [20] Chaudhuri, S. (2001) *Super-Resolution Imaging*. Kluwer Academic Publishers, Norwell, MA, USA.
- [21] Park, S. C., Park, M. K., and Kang, M. K. (2003) Super-resolution image reconstruction : A technical overview. *IEEE Signal Processing Magazine*, **20**, 21–36.
- [22] Jiji, C. V., Chaudhuri, S., and Chatterjee, P. Single frame image super-resolution: Should we process globally or locally? to appear.
- [23] Farsiu, S., Robinson, D., Elad, M., and Milanfar, P. (2004) Advances and challenges in super-resolution. *International Journal of Imaging Systems and Technology*, **14**, 47–57.
- [24] Brown, L. G. (1992) A survey of image registration techniques. *ACM Computing Surveys*, **24**, 325–376.
- [25] Vandewalle, P., Susstrunk, S., and Vetterli, M. (2003) Superresolution images reconstructed from aliased images. In Ebrahimi, T. and Sikora, T. (eds.), *SPIE/IS&T Visual Communication and Image Processing Conference*, Lugano, Switzerland, July, pp. 1398–1405.
- [26] Irani, M. and Peleg, S. (1991) Improving resolution by image registration. *CVGIP: Graph. Models Image Process.*, **53**, 231–239.
- [27] Bertalmio, M., Sapiro, G., Caselles, V., and Ballester, C. (2000) Image inpainting. In Akeley, K. (ed.), *SIGGRAPH 2000, Computer Graphics Proceedings*, New Orleans, USA, July, pp. 417–424. ACM Press / ACM SIGGRAPH / Addison Wesley Longman.
- [28] Masnou, S. (2002) Disocclusion: a variational approach using level lines. *IEEE Transactions on Image Processing*, **11**, 68–76.
- [29] Masnou, S. and Morel, J. (1998) Level lines based disocclusion. *5th IEEE International Conference on Image Processing (3)*, Chicago, USA, October, pp. 259–263. IEEE Computer Society.
- [30] Ballester, C., Bertalmio, M., Caselles, V., Sapiro, G., and Verdera, J. (2001) Filling-in by joint interpolation of vector fields and gray levels. *IEEE Transactions on Image Processing*, **10**, 1200–1211.
- [31] Chan, T. and Shen, J. (2001) Non-texture inpainting by curvature-driven diffusions. *J. Visual Comm. Image Rep.*, **12(4)**, 436–449.
- [32] Oliveira, M. M., Bowen, B., McKenna, R., and Chang, Y.-S. (2001) Fast digital image inpainting. *Proceedings of the IASTED International Conference on Visualization, Imaging and Image Processing (VIIP)*, Marbella, Spain, September, pp. 261–266. ACTA Press.
- [33] Grossauer, H. and Scherzer, O. (2003) Using the complex ginzburg-landau equation for digital inpainting in 2d and 3d. *Scale-Space*, Isle of Skype, UK, June, Lecture Notes on Computer Science, **2695**, pp. 225–236. Springer.
- [34] Borzi, A., Grossauer, H., and Scherzer, O. (2005) Analysis of iterative methods for solving a ginzburg-landau equation. *International Journal of Computer Vision*, **64**, 203–219.
- [35] Hirani, A. H. and Totsuka, T. (1996) Dual domain interaction image restoration : Basic algorithm. *Third IEEE International Conference on Image Processing*, pp. 797–800. IEEE Press.
- [36] Patwardhan, K. A. and Sapiro, G. (2003) Projection based image and video inpainting using wavelets. *IEEE International Conference on Image Processing*, Barcelona, Spain, 14–18, September, pp. 857–860.
- [37] Chan, R., Shen, L., and Shen, Z. (2005) A framelet-based approach to image inpainting. Technical report. Dept. of Mathematics, Chinese University of Hong Kong, Hong Kong.
- [38] Strohmer, T. (1995) On discrete band-limited signal extrapolation. *Mathematical Analysis, Wavelets, and Signal Processing*, **190**, 323–337.
- [39] Grochenig, K. and Strohmer, T. (2001) Numerical and theoretical aspects of non-uniform sampling of band-limited signals. In Marvasti, F. (ed.), *Nonuniform Sampling: Theory and Practice*, chapter 6, pp. 283–324. Kluwer Academic Publishers, Norwell, MA, USA.